The EMBO Journal Vol.18 No.23 pp.6809–6815, 1999

Redox signalling in the chloroplast: structure of oxidized pea fructose-1,6-bisphosphate phosphatase

Mohammed Chiadmi[1,2], Alda Navaza[3], Myroslawa Miginiac-Maslow[4], Jean-Pierre Jacquot[5] and Jacqueline Cherfils[1,6]

[1]Laboratoire d'Enzymologie et Biochimie Structurales, CNRS, Avenue de la Terrasse, 91198 Gif sur Yvette, [2]Laboratoire de Cristallographie et RMN Biologiques, CNRS-EP2075, Faculté de Pharmacie, Université Paris V, 75270 Paris, [3]Laboratoire de Physique, Centre Pharmaceutique, Université de Paris-Sud, 92290 Chatenay-Malabry, [4]Institut de Biotechnologie des Plantes, CNRS, Université de Paris-Sud, 91405 Orsay and [5]Laboratoire de Biologie Forestière, Université de Nancy 1, BP 239, 54506 Vandoeuvre, France

[6]Corresponding author
e-mail: cherfils@lebs.cnrs-gif.fr

Sunlight provides the energy source for the assimilation of carbon dioxide by photosynthesis, but it also provides regulatory signals that switch on specific sets of enzymes involved in the alternation of light and dark metabolisms in chloroplasts. Capture of photons by chlorophyll pigments triggers redox cascades that ultimately activate target enzymes via the reduction of regulatory disulfide bridges by thioredoxins. Here we report the structure of the oxidized, low-activity form of chloroplastic fructose-1,6-bisphosphate phosphatase (FBPase), one of the four enzymes of the Calvin cycle whose activity is redox-regulated by light. The regulation is of allosteric nature, with a disulfide bridge promoting the disruption of the catalytic site across a distance of 20 Å. Unexpectedly, regulation of plant FBPases by thiol–disulfide interchange differs in every respect from the regulation of mammalian gluconeogenic FBPases by AMP. We also report a second crystal form of oxidized FBPase whose tetrameric structure departs markedly from D_2 symmetry, a rare event in oligomeric structures, and the structure of a constitutively active mutant that is unable to form the regulatory disulfide bridge. Altogether, these structures provide a structural basis for redox regulation in the chloroplast.

Keywords: allostery/chloroplast/photosynthesis/redox regulation/thioredoxin

Introduction

Life on earth relies on the assimilation of carbon dioxide by oxygenic photosynthesis in plants and microorganisms. Sunlight provides the energy for the assimilatory reactions, but it also provides regulatory signals that switch on/off specific sets of enzymes involved in the alternation of 'light' and 'dark' metabolisms in the chloroplasts. Reactions activated by light include the synthesis of ATP by the coupling factor ATPase, the reductive pentose phosphate cycle (Calvin cycle) that synthesizes carbohydrates from atmospheric CO_2 (reviewed in Buchanan, 1991; Wolosiuk *et al*., 1993), activation of Rubisco activase (Zhang and Portis, 1999) and, in higher plants, the synthesis of malate by NADP-malate dehydrogenase (MDH). On the other hand, light inactivates only one enzyme of the oxidative pathway, glucose-6-phosphate dehydrogenase. It is now clearly established that light signals are transduced by the ferredoxin–thioredoxin system (reviewed in Jacquot *et al*., 1997a; Ruelland and Miginiac-Maslow, 1999). Capture of photons by chlorophyll pigments in photosystems triggers a redox cascade of disulfide–dithiol interchanges, which ultimately activates target enzymes through the reduction of regulatory disulfide bridges by reduced thioredoxins. The redox-sensitive cysteines in light-regulated chloroplastic enzymes do not display common patterns of organization, suggesting that their regulation will be unique at the atomic level (Ruelland and Miginiac-Maslow, 1999).

The Calvin cycle involves three steps: carboxylation, reduction and regeneration of the key compound ribulose-1,5-bisphosphate. Three out of the four sites of light redox regulation are in the regeneration step: fructose-1,6-bisphosphate phosphatase (FBPase), sedoheptulose-1,7-bisphosphate phosphatase (SBPase) and phosphoribulokinase. The observation that the FBPase-catalyzed reaction, i.e. hydrolysis of fructose-1,6-bisphosphate (F1,6P) into fructose-6-phosphate (F6P), was weak in green algae in the dark and increased markedly after illumination, was among the pioneering evidence that dark–light transitions activate the Calvin cycle (Pedersen *et al*., 1966). The effect is mimicked *in vitro* by the ferredoxin–thioredoxin f system, indicating that redox-active cysteines are involved (Buchanan and Wolosiuk, 1976; Buchanan, 1980). Chloroplastic FBPases indeed differ from their cytosolic counterparts, which are involved in gluconeogenesis and are regulated by AMP in both plants and animals, by a sequence insertion that bears three conserved cysteine residues (Marcus *et al*., 1988; Raines *et al*., 1988). Mutation of any of these cysteines into serine results in constitutively active FBPases, with reduced or no sensitivity to thioredoxins (Jacquot *et al*., 1995, 1997b; Rodriguez-Suarez *et al*., 1997). This established the contribution of the sequence insertion in redox regulation, but whether two or three cysteines are the actual targets of thioredoxin regulation remains unclear (Jacquot *et al*., 1997b; Rodriguez-Suarez *et al*., 1997). Besides disulfide reduction, activation of FBPase also depends on parameters such as light-dependent changes in pH and Mg^{2+} levels (Zimmermann *et al*., 1976).

Gluconeogenic FBPases from mammals have been the subject of extensive crystallographic studies that revealed the structural nature of their allosteric regulation (Ke *et al*., 1990, 1991b; Liang *et al*., 1993; Zhang *et al*., 1993, 1994; Choe *et al*., 1998; Weeks *et al*., 1999). The AMP inhibitor

binds to a site remote from the catalytic site and promotes a marked quaternary change compared with the active form, with one dimer of subunits rotating by 17° relative to the other dimer (Ke *et al*., 1991a; Lipscomb, 1991; Zhang *et al*., 1994). This quaternary reorganization is associated with relatively minor conformational changes at the active site, which retains its overall organization in both inactive (T) and active (R) forms. The only known structure of a chloroplastic FBPase, purified from spinach leaves, displays a quaternary structure that is closer to the T form than to the R form of gluconeogenic FBPases (Villeret *et al*., 1995). Its regulatory insertion is weakly organized and the crystallographic data show no evidence for a disulfide bridge. Here we report the crystal structure of oxidized pea FBPase in two crystal forms, and the crystal structure of a constitutively active mutant. These structures reveal the location of the disulfide bridge within the regulatory insertion and show that it results in a major distortion of the active site. Our results thus explain the allosteric regulation of chloroplastic FBPases by disulfide–dithiol interchange, which we compare with the regulation of gluconeogenic FBPases by AMP. Together with the recently reported structures of chloroplastic MDH (Carr *et al*., 1999; Johansson *et al*., 1999), these structures show that regulation of enzymes by light is achieved by different mechanisms, which gives clues for the regulation of other chloroplastic enzymes and may provide a model for redox regulation in animal cells.

Results

Structures of oxidized wild-type FBPase and of the constitutively active C153S mutant

We report three crystal structures of pea chloroplastic FBPase, all with a tetramer in the asymmetric unit (Figure 1A). The structure of the wild-type enzyme was solved in two crystal forms, which will be referred to as forms I and II. The third structure is a constitutively active mutant in which cysteine 153, in the characteristic insertion of chloroplastic FBPase, has been replaced by a serine residue. Both wild-type forms show clear electron density for a disulfide bridge between Cys153 and Cys173 in the insertion (Figure 1B). The insertion has an extended conformation from Pro149 to Asp156 and forms an α-helix from Thr168 to Cys178, but most intervening residues are disordered in all monomers except one in form I. The third conserved cysteine residue in the insertion, Cys178, is on the buried side of the helix (Figure 1B). Two other cysteine side chains (Cys49 and Cys190) are close in the FBPase core but show no density for a disulfide bridge, in agreement with mutagenesis studies which showed that neither of them influences the regulation by thioredoxin (Jacquot *et al*., 1997b; Rodriguez-Suarez *et al*., 1997). Thus, the redox-sensitive cysteines are located in the insertion and both crystal forms correspond to the oxidized, inactive form of chloroplastic FBPase. The regulatory cysteines are separated by a loop whose length varies from 14 to 19 amino acids among FBPase species.

Amino acids that form the active site are almost invariant between chloroplastic and gluconeogenic FBPases. We thus identify the active site in pea FBPase as that characterized in pig kidney FBPase by crystallographic studies (Zhang *et al*., 1993; Choe *et al*., 1998). Asn237, Tyr269, Tyr289 and Arg268 (Asn212, Tyr244, Tyr264 and Arg243 in pig), which bind the 6-phosphate of F1,6P, and Lys299 (Lys274 in pig), which binds the fructose, superimpose almost exactly to their counterparts in pig kidney FBPase, while Asp129, Gly130 and Arg301 (Asp118, Gly119 and Arg276 in pig), which bind the 1-phosphate, display only moderate displacements. In contrast, we observe a dramatic conformational change that affects Glu105 (Glu97 in pig kidney FBPase), a critical ligand of the catalytic divalent ions (Chen *et al*., 1993; Zhang *et al*., 1993). The movement spans residues 95–118, which form strands β1 and β2 of the N-terminal domain β-sheet (Figure 2A and C). The two strands move inwards towards the catalytic site by 8–9 Å. This movement removes Glu105 from its position in the active site and introduces the hydrophobic side chain of Val109 close to the first and second cation binding sites (Figure 2D). Moreover, this conformation of the loop between strands β1 and β2 would conflict with the position of the 70's loop that engages the active site in the F6P–P_i product complex (Figure 2C and D) (Choe *et al*., 1998). As a result, the contours of the active site in oxidized FBPase are not compatible with the binding of the catalytic metal ions.

This conformational change directly involves the insertion, which packs against strands β1 and β2 opposite to the active site and thereby stabilizes the inactive conformation of the active site across a distance of 20 Å (Figure 2A). This is in marked contrast to the structure of chloroplastic spinach FBPase, where the insertion is flexible in the solvent and does not display a disulfide bridge, and the active site configuration resembles that of pig kidney FBPase (Figure 2B) (Villeret *et al*., 1995). In addition, strands β1 and β2 are exchanged in oxidized pea FBPase compared with spinach and mammalian FBPases, thus forming an antiparallel N-terminal β-sheet (Figure 2).

The regulatory disulfide bridge between cysteines 153 and 173 cannot be formed in the C153S mutant, which is active irrespective of dithiothreitol (DTT) and thioredoxin f (Jacquot *et al*., 1997b; Rodriguez-Suarez *et al*., 1997). The C153S FBPase is isomorphous to wild-type form I FBPase, from which it differs only in the insertion. The insertion retains the helical conformation from Thr168 to Cys178, but its N-terminal part, including Ser153, is less well defined and has shifted apart by 2 Å on average (Figure 3). Surprisingly, strands β1 and β2 have the conformation of oxidized wild-type FBPase, which suggests that the active site is not functional in this crystal structure. The C153S mutant can thus adopt the conformation of oxidized, inactive wild-type FBPase.

The quaternary structure of oxidized FBPase

Allosteric regulation of pig kidney FBPase by AMP involves a quaternary structure change that affects the orientation of one dimer relative to the other (Ke *et al*., 1991a; Zhang *et al*., 1994). No quaternary rearrangements are observed between oxidized pea FBPase (form I) and spinach FBPase, despite the dramatic tertiary changes at the insertion and the active site. In contrast, oxidized form II FBPase has a different quaternary structure. However, individual dimers of form I and II are essentially the same except at the dimer–dimer interface, where side chain adjustments allow that most interactions are

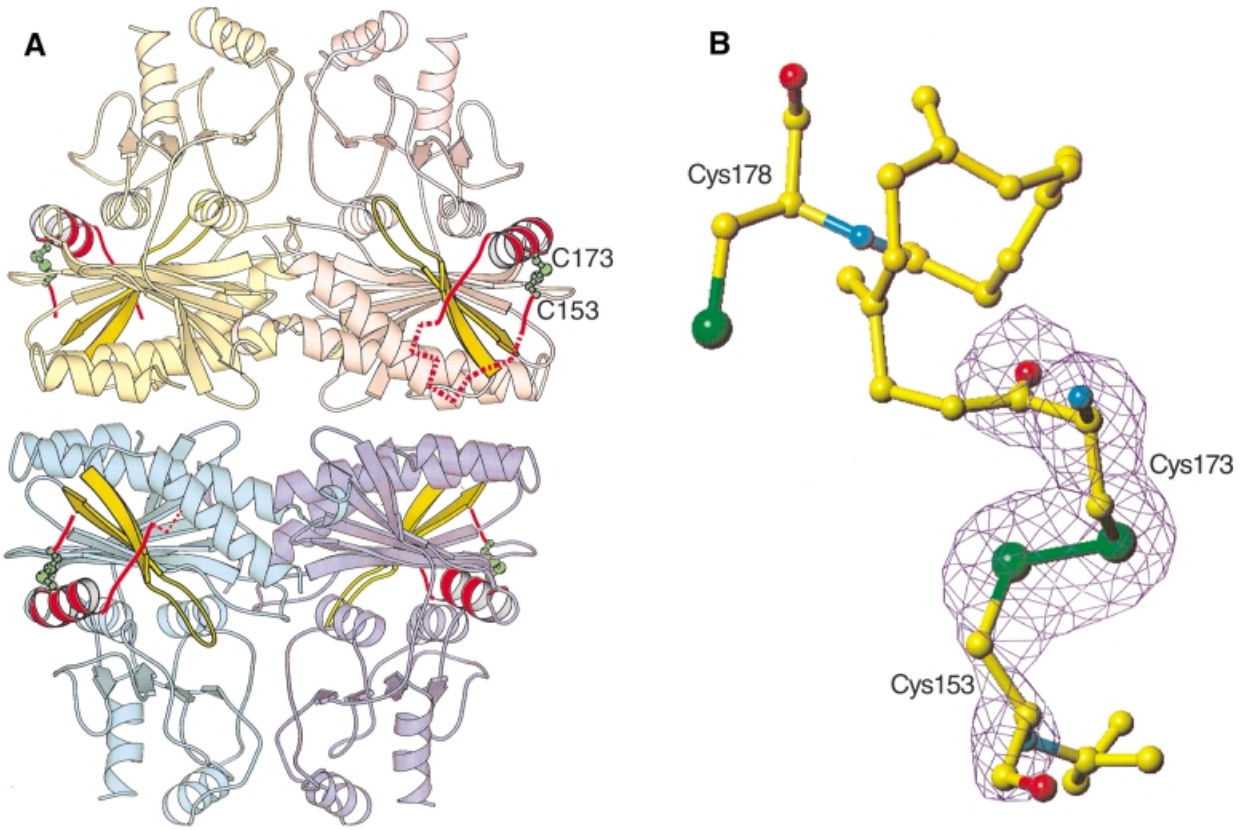

Fig. 1. Structure of oxidized FBPase. (**A**) The wild-type form I FBPase tetramer. The insertion (residues 153–173) is in red, the disulfide bridge in green, strands β1 and β2 (residues 99–118) in yellow. Dashed lines indicate regions of weak electron density. The dimers are in light pink/yellow and in shades of blue. (**B**) The disulfide bridge between Cys153 and Cys173. $|F_o| - |F_c|$ electron density of wild-type form I FBPase with the disulfide bridge omitted from the calculation, shown at 5σ cutoff. Residues 152 and 174–177 from the insertion are shown as main chain trace. Cys178 is located on the side of the helix that faces the core of the enzyme.

common. In wild-type form I, the dimers are related by an ~2-fold symmetry. In form II, the tetramer shows a marked departure from D_2 symmetry, with a deviation of 9° from 2-fold symmetry and a translation of 3.5 Å in the plane of the dimer–dimer interface (Figure 4). Early experiments on chloroplastic FBPases suggested that a tetramer-to-dimer transition occurs at alkaline pH (Pradel *et al*., 1981). We checked whether the enzyme is a tetramer in solution by ultracentrifugation at pH 7, which corresponds to the pH of chloroplast in the dark, and at pH 8.5 in the presence of the reducing agent Tris-(2-carboxyethyl)phosphine hydrochloride (TCEP), F6P and Mg^{2+}, which should mimic light conditions. Both wild-type FBPase and the C153S mutant had the sedimentation constant expected for a tetramer, regardless of the pH. There is thus no evidence, in our hands, that allosteric activation promotes dissociation of the tetramer into dimers. The ability of the dimer–dimer interface of pea FBPase to buckle may be best explained by its slightly more hydrophobic character and a slightly smaller surface area compared with the pig kidney enzyme, both imposing less orientational constraint on the interface. Consequently the allosteric regulation may target the dimer rather than the tetramer, as is indeed suggested by the cooperativity Hill number of 2 for F1,6P and Mg^{2+} (Jacquot *et al*., 1995). A departure from point group symmetry was seldom observed in oligomeric proteins, with the notable exception of yeast hexokinase, in which case monomer–dimer equilibrium was involved (Steitz *et al*., 1976). It is, however, not unprecedented that allosteric proteins can visit more than two quaternary structures, as in the case of Ypsilanti hemoglobin (Smith *et al*., 1991) or aspartate transcarbamylase (Cherfils *et al*., 1987).

Discussion

Structural basis for the redox regulation of chloroplastic FBPase

Our structures reveal that a disulfide bridge forms between Cys153 and Cys173 in the insertion, resulting in a disorder-to-order transition at the insertion compared with the structure of chloroplastic spinach FBPase (Villeret *et al*., 1995). This conformation stabilizes an altered conformation of β-strands β1 and β2, which slide by 8–9 Å in towards the active site and disrupt the binding sites for the catalytic Mg^{2+} cations 20 Å away from the disulfide bridge. The structure of spinach FBPase displays no evidence for a disulfide bridge, and the organization of its active site resembles that of either the T or R forms of gluconeogenic FBPases (Ke *et al*., 1990, 1991b; Liang *et al*., 1993; Zhang *et al*., 1993, 1994; Choe *et al*., 1998). We surmise therefore that this structure is close to the active, reduced FBPase. The comparison of our oxidized FBPase structures with that of spinach and pig suggests that upon reduction of the disulfide bridge by thioredoxin, the secondary structure of the insertion melts and releases the β1–β2 strands. This

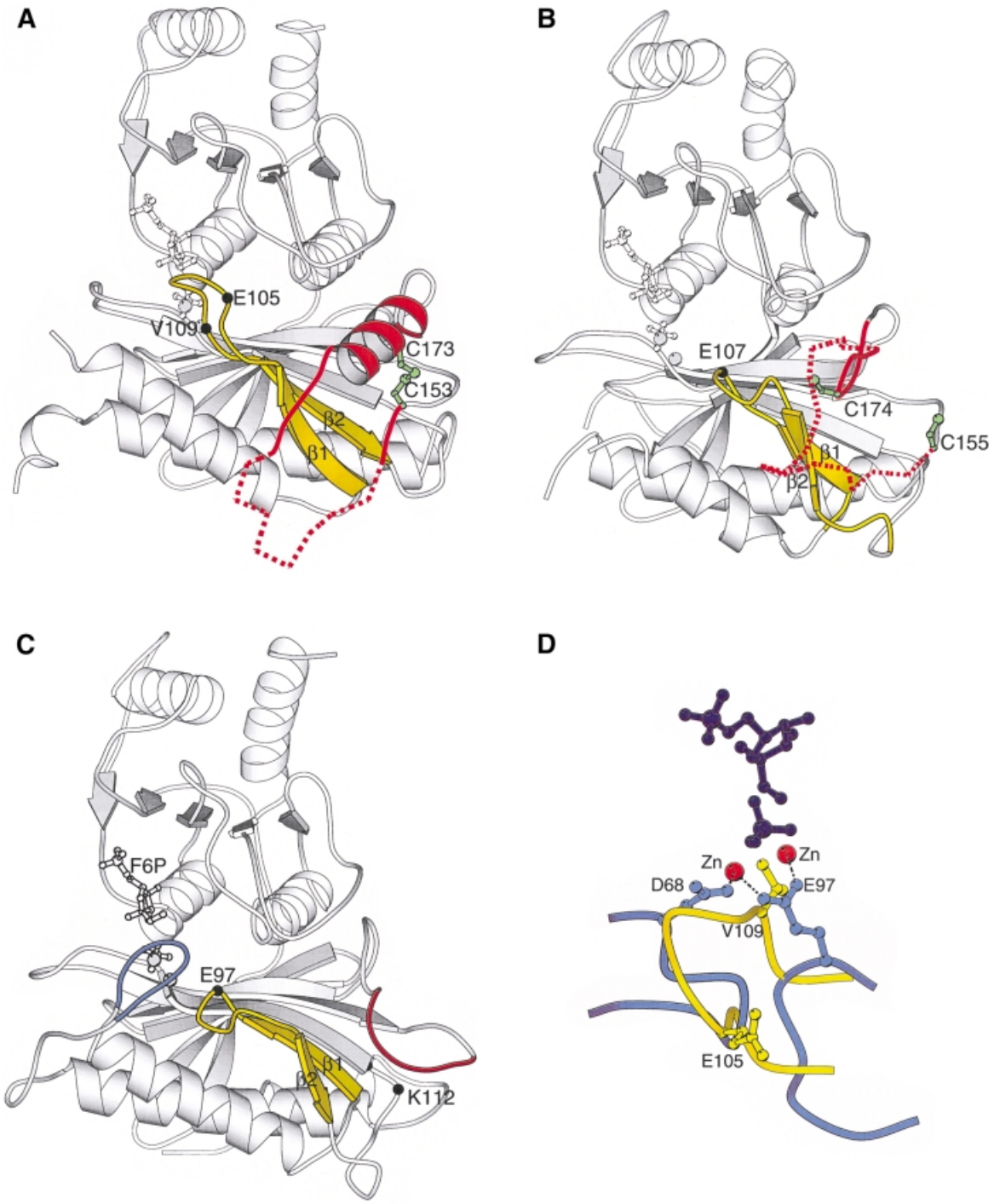

Fig. 2. Comparison of oxidized pea FBPase to pig kidney and spinach FBPases. (**A**) Oxidized form I pea FBPase. (**B**) Chloroplastic spinach FBPase (PDB entry code 1SPI) (Villeret *et al*., 1995). (**C**) R form gluconeogenic pig kidney FBPase in complex with F6P, P_i and Zn^{2+} (PDB entry code 1CNQ) (Choe *et al*., 1998). (**D**) Close-up view of the cation binding site with pig kidney FBPase shown in blue, cations in red and oxidized pea FBPase in yellow. Orientation and colour coding in (A), (B) and (C) are as in Figure 1A. The location of the active site in pea and spinach FBPases is indicated by a model of F6P, P_i and Zn^{2+} shown as dashed lines. The 70's loop in pig kidney FBPase is in blue. The corresponding loop is disordered in pea and spinach FBPases. The loop in pig kidney FBPase that corresponds to the chloroplastic insertion is in red. The binding site for AMP in pig kidney FBPase is indicated by one of its ligands, Lys112. The close-up view in (D) shows that the interaction of the 70's loop and the loop between strands β1 and β2 with the cations in pig FBPase, is prevented by the inwards movement of strands β1and β2 in oxidized pea FBPase. This movement places Val109 near the location of the cation binding site and removes Glu105, which corresponds to Glu97 in pig kidney FBPase, from the active site.

allows the β-strands to move back upon substrate binding so that the active site adopts its catalytically-competent conformation. We also observed that the topology of the β-strands is exchanged in our structures compared with spinach and pig FBPases, yielding an antiparallel β-sheet topology. The antiparallel topology may not have been identified in spinach FBPase due to its lower resolution (Villeret *et al*., 1995). Alternatively, an actual β-strand interchange may have occurred in oxidized pea FBPase. The backwards movement of the β-strands, which projects addi-

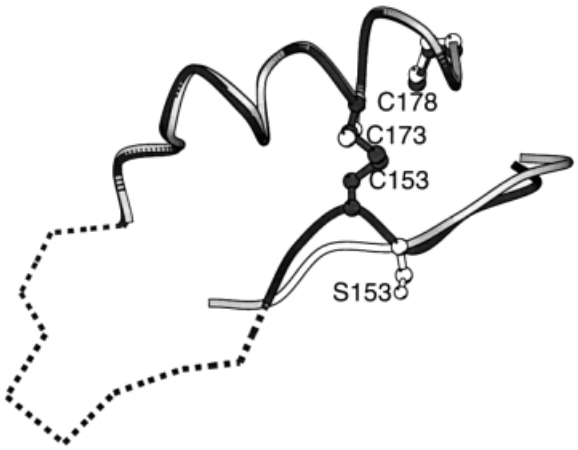

Fig. 3. The insertion in wild-type form I (dark grey) and in the Cys173Ser mutant (light grey). Residues 155–168 are weakly defined in the electron density of form I (dashed lines) and cannot be traced in the C173S mutant.

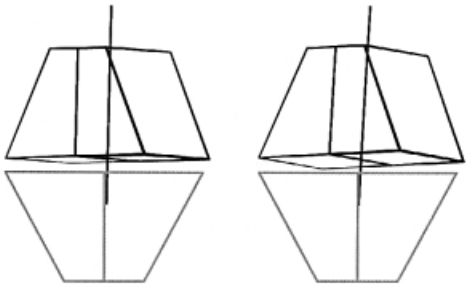

Fig. 4. The quaternary structures of wild-type form I (left) and wild-type form II (right) FBPases. The reference dimer (in grey) has the same orientation in both forms. The 2-fold axis relating monomers of the top dimer is shown. Wild-type form I has D_2 symmetry. In form II, the top dimer is rotated by 170° relative to the bottom dimer and is translated by 3.5 Å in the plane of the dimer–dimer interface.

tional residues at the dimer–dimer interface, would thus be accommodated by the β-strand interchange, which requires that connecting loops are longer (Figures 1 and 2). β-strand disruption and reorganization is not unprecedented, as recently observed upon activation of the GTP-binding protein Arf by GTP (Goldberg, 1998).

The role of conserved cysteines was anticipated by sequence analysis (Marcus *et al*., 1988) and mutagenesis studies in pea and spinach FBPase (Jacquot *et al*., 1995, 1997b; Rodriguez-Suarez *et al*., 1997). Surprisingly, only the C153S mutant was found to be constitutively active, whereas both the C173S and C178S mutants were still weakly activated by thioredoxin and DTT (Jacquot *et al*., 1997b; Rodriguez-Suarez *et al*., 1997). Our structures provide a framework to reconcile these conflicting observations. First, the structure of the C153S mutant shows that the insertion has moved backwards compared with wild-type oxidized FBPase, bringing Ser153 closer to Cys178 (Figure 3), a movement that could occur in the C173S mutant as well. Cys153 could thus form an artefactual disulfide bridge with Cys178 in the C173S mutant. Secondly, our structures demonstrate that the C153S mutant can adopt the inactive conformation, suggesting that this and other mutants are in equilibrium between an inactive and an active conformation. Since Cys178 is buried in oxidized FBPase, its mutation to serine could perturb the conformation of the insertion, and thereby shift the equilibrium towards the active form. This readily explains the basal activity of the C173S and C178S mutants. The kinetics of the C153S mutant, which is constitutively active (Jacquot *et al*., 1997b; Rodriguez-Suarez *et al*., 1997), are best explained by a rapid shift of the equilibrium in the presence of the substrate and Mg^{2+}, which would require fast-flow kinetics to detect.

The redox regulation of chloroplastic FBPase is distinct from the one that was recently described for malate dehydrogenase (Carr *et al*., 1999; Johansson *et al*., 1999). In MDH, redox-sensitive cysteines are carried by a C-terminal extension. Dark-driven oxidation locks the extension inside the active site, where it acts as an internal inhibitor. In contrast, the regulatory insertion in FBPase does not interact directly with the active site, but it stabilizes its inactive conformation. This could explain why oxidized FBPase retains a low basal activity, whereas oxidized MDH is totally inactive. In both structures however, the redox-sensitive cysteines are remote from the active site and accessible to thioredoxins at the surface of the enzyme. This may also be the case for SBPase, another light-regulated enzyme of the Calvin cycle. SBPase is closely related to FBPase, but its regulatory cysteines are located in a loop equivalent to the 70's loop, and it lacks the regulatory insertion (Dunford *et al*., 1998). We suggest that oxidation of the 70's loop in SBPase could fulfil a role analogous to that of the FBPase insertion, by acting on the nearby β-strands.

Allosteric regulation of FBPase in photosynthesis and gluconeogenesis: dithiol–disulfide interchange versus AMP binding

Allosteric regulation of FBPase opposes redox signals in chloroplastic species to AMP concentration signals in both plants and animals gluconeogenic species. Comparison of the corresponding X-ray structures shows that the structural bases for allosteric regulation differ in almost every aspect between the two FBPase classes. First, the binding site for AMP in gluconeogenic FBPase is close to, but distinct from, the location of the redox-sensitive insertion in chloroplastic FBPases. The site does not exist in chloroplastic FBPase, where the adenine site is obstructed by Ile33 and the phosphate is mimicked by Asp34. Secondly, the AMP binding site involves dimer–dimer interface residues, whereas the insertion forms no contact with other subunits. Thirdly and most importantly, AMP promotes large quaternary changes associated with only minor changes within the active site. In contrast, redox regulation induces a major disruption of the active site and presumably little quaternary rearrangements. The latter point, however, will have to be confirmed by the structure of reduced FBPase. These different means nonetheless achieve the same result, which is the disruption of the catalytic Mg^{2+} binding sites. This is consistent with the observation that oxidized FBPase can be activated without reduction by high Mg^{2+} concentrations (Schurmann and Wolosiuk, 1978). Both regulatory mechanisms displace the same glutamate residue (Glu105 in pea and Glu97 in pig) although the displacements are of different amplitudes. However, pea FBPase is unique in using a hydrophobic side chain, Val109, to block the Mg^{2+} binding sites, a configuration reminiscent of a leucine residue that binds near the Mg^{2+} binding site of Ras in the Ras–Sos complex (Boriack-Sjodin *et al*., 1998). Since the β1–β2 strands are another close route from the AMP binding site to the active site, it would be interesting to

investigate whether they are involved in the transmission of the allosteric signal in gluconeogenic FBPases as well.

Redox signalling by thioredoxins

One of the functions of the activation of Calvin cycle enzymes by light is probably to avoid futile or incomplete cycles and/or reverse reactions to occur in the dark when the supply of substrates is limiting (Buchanan, 1991). Besides, the generation of reducing power by the photosynthetic electron flow in a functional chloroplast in the light is concomitant with the build-up of high oxygen concentrations by the Calvin cycle enzymes. Thus, it was suggested recently that redox regulation in the chloroplast may have also evolved as a defence against photosynthetic oxidative stress, being correlated with the appearance of oxygenic photosynthesis (Ruelland and Miginiac-Maslow, 1999). Both roles appear to be compatible with our FBPase structures. Oxidation of FBPase clearly impairs catalysis, as it stabilizes a conformation of the active site that is not compatible with the catalytic reaction. In addition, we observe that both wild-type FBPase and the redox-insensitive mutant adopt the inactive conformation in the absence of substrate. This suggests that the thioredoxin-sensitive disulfide bridge stabilizes rather than promotes the inactive conformation, and that this conformation prevails in the absence of either the substrate or the redox signal. This supports the hypothesis that a role of thioredoxin could be to sustain the catalytic, reduced conformation of FBPase by successive reduction cycles in order to counterbalance the oxidative environment generated by daylight conditions.

The chloroplast provides a particular environment where oxidative conditions coexist with the reductive conditions prevailing in other cellular compartments. As such, redox regulation in the chloroplast bears analogies to redox regulation in animal cells under conditions of oxidative stress. Recent evidence suggests that reactive oxygen species such as H_2O_2 are likely to be involved as signal transduction messengers in the regulation of gene transcription (reviewed in Sen and Packer, 1996; Kamata and Hirata, 1999) and apoptosis (Saitoh *et al*., 1998) by thioredoxins. In particular, thioredoxins have been shown to modulate the activity of transcription factors, including NF-κB, whose redox-sensitive cysteine is located in a loop that recognizes DNA (Muller *et al*., 1995; Qin *et al*., 1995; Hirota *et al*., 1999), and in the activation of apoptosis signal-regulating kinase 1 (Saitoh *et al*., 1998). Our FBPase structures, as well as the recently described structure of oxidized chloroplastic MDH (Carr *et al*., 1999; Johansson *et al*., 1999), provide examples of redox regulation in an oxidative environment, allowing a protein to keep its disulfide bridges reduced under high oxygen concentration. Importantly, they also show that redox-sensitive regulatory cysteines are well suited for long-distance regulatory effects, providing an external site accessible for reduction by thioredoxins, which can be remote from the possibly less accessible site where the regulatory action is to be exerted. As such they may provide a useful model for redox regulation in animal cells, where structural information is scarce at the moment.

Materials and methods

Crystallization and structure determination

Recombinant wild-type FBPase from pea, and a mutant where Cys153 in the insertion was replaced by Ser (C153S), were expressed and purified as described (Jacquot *et al*., 1995, 1997b). Crystals were grown in hanging drops. Two crystal forms were obtained for the wild-type enzyme. Form I crystals grew in 25% PEG 400, 50 mM sodium acetate pH 5, 50 mM $MgCl_2$ and 5 mM F6P. Form II crystals were obtained under the same conditions as form I, except that 5 mM reducing agent TCEP was added to the crystallization buffer. Crystals of the C153S mutant were obtained in 18–20% PEG 1000, 50 mM sodium acetate pH 5, 50 mM $MgCl_2$ and 5 mM F6P.

Table I. X-ray structure determination

	Wild-type form I	Wild-type form II	C153S
Space group	$P2_1$	$P2_1$	$P2_1$
Unit cell *a*,*b*,*c* (Å)	78.9, 113.9, 94.8	71.6, 126.3, 78.0	78.9, 114.5, 94.5
β (°)	114.4	97.7	114.5
Measured reflections	242800	344547	291800
Unique reflections	53083	69334	41127
Completeness (%)	89	99	88
Resolution range (Å)	24–2.4	24–2.2	18–2.6
R_{sym}	4.5	6.7	9.6
R-factor (%)	18.6	19.8	23.5
R_{free} (%)	23.6	24.7	29.1
R.m.s.d. bond length (Å)	0.008	0.018	0.009
R.m.s.d. bond angles (°)	1.36	2.5	1.36
No. of atoms	9906	9920	9750
No. of water molecules	330	195	0

Parameters and statistics for structure determination are given in Table I. Diffraction data were recorded at the LURE synchrotron on beam line W32 (λ = 0.965 Å) and D41 (λ = 1.375 Å). Diffraction intensities were processed with DENZO (Otwinowski, 1993). All crystal forms contain a tetramer in the asymmetric unit. A dimer of spinach FBPase (Villeret *et al*., 1995) (PDB entry 1SPI), with the insertions removed, was used as a model for molecular replacement of wild-type form I using AMoRe (Navaza, 1994). A model of the tetramer was then built by quadruplicating monomer A according to the highest correlation solution. At that stage, maps showed an important departure from the spinach enzyme, extending from the regulatory loop to the active site. Strict non-crystallographic symmetry was applied at the initial stages of rebuilding, and subsequently released. Graphical building was carried out with O (Jones *et al*., 1991), in alternation with conventional refinement and simulated annealing with X-Plor (Brünger *et al*., 1989). The structure of wild-type form II was solved by molecular replacement using partially refined wild-type form I. A solution was obtained with two dimers, whereas no solution with a high correlation was obtained with the tetramer. Building was carried out essentially with TURBO (Roussel,A., Inisan,A.G. and Cambillau,C., AFMB and BioGraphics, Marseille, France), refinement with X-Plor without non-crystallographic constraints and during the last stages with the maximum-likelihood refinement program REFMAC (CCP4, 1994). Crystals of the C153S mutant are isomorphous to wild-type form I. The structure of the C153S mutant was solved by Fourier maps, using the phases from partially refined form I. Coordinates and structure factors have been deposited in the PDB with entry codes 1D9Q, 1DCU and 1DBZ.

Neither of these structures has electron density for the N-terminus (residues 1–15) and for the loop between residues 65–75, and residues 158–164 in the insertion are traced in only one chain of wild-type form I. These regions were not proteolyzed in wild-type FBPase as assessed by N-terminal sequencing of the stock solution and by SDS–PAGE of dissolved crystals, which showed a single band at the expected molecular weight. The oligomeric state of wild-type FBPase and the C153S mutant was analyzed by sedimentation velocity at 40 000 r.p.m.

Acknowledgements

We thank Roger Fourme, Javier Perez and Anita Lewitt-Bentley for making beam lines W32 and D41 at the LURE synchrotron centre available to us; Diep Lê (LEBS) for N-terminal sequencing and Gérard Batelier (LEBS) for ultracentrifugation; J.Janin, B.Olofsson and A.Sanson for critical reading of the manuscript.

References

Boriack-Sjodin,P.A., Margarit,S.M., Bar-Sagi,D. and Kuriyan,J. (1998) The structural basis of the activation of Ras by Sos. *Nature*, **394**, 337–343.

Brünger,A.T., Karplus,M. and Petsko,G.A. (1989) Crystallographic refinement by simulated annealing: application to crambin. *Acta Crystallogr. A*, **45**, 50–61.

Buchanan,B.B. (1980) Role of light in the regulation of chloroplast enzymes. *Annu. Rev. Plant Physiol.*, **31**, 341–374.

Buchanan,B.B. (1991) Regulation of CO_2 assimilation in oxygenic photosynthesis: the ferredoxin/thioredoxin system. Perspective on its discovery, present status and future development. *Arch. Biochem. Biophys.*, **288**, 1–9.

Buchanan,B.B. and Wolosiuk,R.A. (1976) Photosynthetic regulatory protein found in animal and bacterial cells. *Nature*, **264**, 669–670.

Carr,P.D., Verger,D., Ashton,A.R. and Ollis,D.L. (1999) Chloroplast NADP-malate dehydrogenase: structural basis of light-dependent regulation of activity by thiol oxidation and reduction. *Structure*, **7**, 461–475.

CCP4 (1994) The CCP4 suite: program for protein crystallography. *Acta Crystallogr. D*, **50**, 760–763.

Chen,L., Hegde,R., Chen,M. and Fromm,H.J. (1993) Site-specific mutagenesis of the metal binding sites of porcine fructose-1,6-bisphosphatase. *Arch. Biochem. Biophys.*, **307**, 350–354.

Cherfils,J., Vachette,P., Tauc,P. and Janin,J. (1987) The pAR5 mutation and the allosteric mechanism of *Escherichia coli* aspartate carbamoyltransferase. *EMBO J.*, **6**, 2843–2847.

Choe,J.Y., Poland,B.W., Fromm,H.J. and Honzatko,R.B. (1998) Role of a dynamic loop in cation activation and allosteric regulation of recombinant porcine fructose-1,6-bisphosphatase. *Biochemistry*, **37**, 11441–11450.

Dunford,R.P., Durrant,M.C., Catley,M.A. and Dyer,T.A. (1998) Location of the redox-active cysteines in chloroplast sedoheptulose-1,7-bisphophatase indicates that its allosteric regulation is similar but not identical to that of fructose-1,6-bisphosphatase. *Photosynth. Res.*, **58**, 221–230.

Goldberg,J. (1998) Structural basis for activation of ARF GTPase: mechanisms of guanine nucleotide exchange and GTP–myristoyl switching. *Cell*, **95**, 237–248.

Hirota,K., Murata,M., Sachi,Y., Nakamura,H., Takeuchi,J., Mori,K. and Yodoi,J. (1999) Distinct roles of thioredoxin in the cytoplasm and in the nucleus. A two-step mechanism of redox regulation of transcription factor NF-κB. *J. Biol. Chem.*, **274**, 27891–27897.

Jacquot,J.P. *et al*. (1995) High-level expression of recombinant pea chloroplast fructose-1,6-bisphosphatase and mutagenesis of its regulatory site. *Eur. J. Biochem.*, **229**, 675–681.

Jacquot,J.P., Lancelin,J.M. and Meyer,Y. (1997a) Thioredoxins: structure and function in plant cells. *New Phytol.*, **136**, 543–570.

Jacquot,J.P., Lopez-Jaramillo,J., Miginiac-Maslow,M., Lemaire,S., Cherfils,J., Chueca,A. and Lopez-Gorge,J. (1997b) Cysteine-153 is required for redox regulation of pea chloroplast fructose-1,6-bisphosphatase. *FEBS Lett.*, **401**, 143–147.

Johansson,K., Ramaswamy,S., Saarinen,M., Lemaire-Chamley,M., Issakidis-Bourguet,E., Miginiac-Maslow,M. and Eklund,H. (1999) Structural basis for light activation of a chloroplast enzyme: the structure of sorghum NADP-malate dehydrogenase in its oxidized form. *Biochemistry*, **38**, 4319–4326.

Jones,T.A., Zou,J.-Y., Cowan,S.W. and Kjeldgaard,M. (1991) Improved methods for building protein models in electron density maps and the location of errors in these models. *Acta Crystallogr. A*, **47**, 110–119.

Kamata,H. and Hirata,H. (1999) Redox regulation in cellular signalling. *Cell. Signal.*, **11**, 1–14.

Ke,H.M., Zhang,Y.P. and Lipscomb,W.N. (1990) Crystal structure of fructose-1,6-bisphosphatase complexed with fructose 6-phosphate, AMP and magnesium. *Proc. Natl Acad. Sci. USA*, **87**, 5243–5247.

Ke,H.M., Liang,J.Y., Zhang,Y.P. and Lipscomb,W.N. (1991a) Conformational transition of fructose-1,6-bisphosphatase: structure comparison between the AMP complex (T form) and the fructose 6-phosphate complex (R form). *Biochemistry*, **30**, 4412–4420.

Ke,H.M., Zhang,Y.P., Liang,J.Y. and Lipscomb,W.N. (1991b) Crystal structure of the neutral form of fructose-1,6-bisphosphatase complexed with the product fructose 6-phosphate at 2.1-Å resolution. *Proc. Natl Acad. Sci. USA*, **88**, 2989–2993.

Liang,J.Y., Zhang,Y., Huang,S. and Lipscomb,W.N. (1993) Allosteric transition of fructose-1,6-bisphosphatase. *Proc. Natl Acad. Sci. USA*, **90**, 2132–2136.

Lipscomb,W.N. (1991) Structure and function of allosteric enzymes. *Chemtracts Biochem. Mol. Biol.*, **2**, 1–15.

Marcus,F., Moberly,L. and Latshaw,S.P. (1988) Comparative amino acid sequence of fructose-1,6-bisphosphatases: identification of a region unique to the light-regulated chloroplast enzyme. *Proc. Natl Acad. Sci. USA*, **85**, 5379–5383.

Muller,C.W., Rey,F.A., Sodeoka,M., Verdine,G.L. and Harrison,S.C. (1995) Structure of the NF-κB p50 homodimer bound to DNA. *Nature*, **373**, 311–317.

Navaza,J. (1994) AMoRe: an automated package for molecular replacement. *Acta Crystallogr. A*, **50**, 157–163.

Otwinowski,Z. (1993) Oscillation data reduction program. In Sawyer,L., Isaacs,N. and Bailey,S. (eds), *CCP4 Study Weekend: Data Collection and Processing*. Daresbury Laboratory, Warrington, UK, pp. 56–62.

Pedersen,T.A., Kirk,M. and Bassham,J. (1966) Light–dark transients in levels of intermediate compounds during photosynthesis in air adapted *Chlorella. Physiol. Plant.*, **19**, 219–231.

Pradel,J., Soulie,J.M., Buc,J., Meunier,J.C. and Ricard,J. (1981) On the activation of fructose-1,6-bisphosphatase of spinach chloroplasts and the regulation of the Calvin cycle. *Eur. J. Biochem.*, **113**, 507–511.

Qin,J., Clore,G.M., Kennedy,W.M., Huth,J.R. and Gronenborn,A.M. (1995) Solution structure of human thioredoxin in a mixed disulfide intermediate complex with its target peptide from the transcription factor NF-κB. *Structure*, **3**, 289–297.

Raines,C.A., Lloyd,J.C., Longstaff,M., Bradley,D. and Dyer,T. (1988) Chloroplast fructose-1,6-bisphosphatase: the product of a mosaic gene. *Nucleic Acids Res.*, **16**, 7931–7942.

Rodriguez-Suarez,R.J., Mora-Garcia,S. and Wolosiuk,R.A. (1997) Characterization of cysteine residues involved in the reductive activation and the structural stability of rapeseed (*Brassica napus*) chloroplast fructose-1,6-bisphosphatase. *Biochem. Biophys. Res. Commun.*, **232**, 388–393.

Ruelland,E. and Miginiac-Maslow,M. (1999) Regulation of chloroplast enzyme activities by thioredoxins: activation or relief from inhibition? *Trends Plant Sci.*, **4**, 136–141.

Saitoh,M., Nishitoh,H., Fujii,M., Takeda,K., Tobiume,K., Sawada,Y., Kawabata,M., Miyazono,K. and Ichijo,H. (1998) Mammalian thioredoxin is a direct inhibitor of apoptosis signal-regulating kinase (ASK) 1. *EMBO J.*, **17**, 2596–2606.

Schurmann,P. and Wolosiuk,R.A. (1978) Studies on the regulatory properties of chloroplast fructose-1,6-bisphosphatase. *Biochim. Biophys. Acta*, **522**, 130–138.

Sen,C.K. and Packer,L. (1996) Antioxidant and redox regulation of gene transcription. *FASEB J.*, **10**, 709–720.

Smith,F.R., Lattman,E.E. and Carter,C.W.,Jr (1991) The mutation β99 Asp–Tyr stabilizes Y–a new, composite quaternary state of human hemoglobin. *Proteins*, **10**, 81–91.

Steitz,T.A., Fletterick,R.J., Anderson,W.F. and Anderson,C.M. (1976) High resolution X-ray structure of yeast hexokinase, an allosteric protein exhibiting a non-symmetric arrangement of subunits. *J. Mol. Biol.*, **104**, 197–222.

Villeret,V., Huang,S., Zhang,Y., Xue,Y. and Lipscomb,W.N. (1995) Crystal structure of spinach chloroplast fructose-1,6-bisphosphatase at 2.8 Å resolution. *Biochemistry*, **34**, 4299–4306.

Weeks,C.M., Roszak,A.W., Erman,M., Kaiser,R., Jornvall,H. and Ghosh,D. (1999) Structure of rabbit liver fructose 1,6-bisphosphatase at 2.3 Å resolution. *Acta Crystallogr. D Biol. Crystallogr.*, **55**, 93–102.

Wolosiuk,R.A., Ballicora,M.A. and Hagelin,K. (1993) The reductive pentose phosphate cycle for photosynthetic CO_2 assimilation: enzyme modulation. *FASEB J.*, **7**, 622–637.

Zhang,N. and Portis,A.R.,Jr (1999) Mechanism of light regulation of rubisco: a specific role for the larger rubisco activase isoform involving reductive activation by thioredoxin-f. *Proc. Natl Acad. Sci. USA*, **96**, 9438–9443.

Zhang,Y., Liang,J.Y., Huang,S., Ke,H. and Lipscomb,W.N. (1993) Crystallographic studies of the catalytic mechanism of the neutral form of fructose-1,6-bisphosphatase. *Biochemistry*, **32**, 1844–1857.

Zhang,Y., Liang,J.Y., Huang,S. and Lipscomb,W.N. (1994) Toward a mechanism for the allosteric transition of pig kidney fructose-1,6-bisphosphatase. *J. Mol. Biol.*, **244**, 609–624.

Zimmermann,G., Kelly,G.J. and Latzko,E. (1976) Efficient purification and molecular properties of spinach chloroplast fructose-1,6-bisphosphatase. *Eur. J. Biochem.*, **70**, 361–367.

Received September 29, 1999; revised and accepted October 15, 1999